Variations of the residual circulation in the Northern Hemispheric winter

S. Tegtmeier,[1,2] K. Krüger,[1,3] I. Wohltmann,[1] K. Schoellhammer,[1] and M. Rex[1]

[1]   A multiyear time series of the vortex-averaged diabatic descent for 47 Arctic winters from 1957/1958 until 2003/2004 is presented. The climatology of diabatic descent is based on trajectory calculations coupled with diabatic heating rate calculations carried out in the polar lower stratosphere of the Northern Hemisphere winters. We demonstrate the improved performance of the approach based on diabatic heating rates compared to the approach based on vertical winds from meteorological analysis. The time series of the vortex-averaged diabatic descent gives a detailed picture of intensity and altitude dependence of the stratospheric vertical transport processes during the Arctic winter. In addition to the overall vortex-averaged diabatic descent, the spatial structure of the descent is analyzed for two different Arctic winters. We demonstrate for this case study that not only the intensity but also the zonal structure of the diabatic descent depends on the meteorological conditions in the polar vortex. The climatology is characterized by very pronounced interannual variability which is linked to the variability of temperature anomalies and to the variability of Eliassen-Palm (EP)-flux anomalies, wherein strong planetary wave activity leads to strong diabatic descent and vice versa. The correlation between EP-flux and descent shows that tropospheric dynamics have a strong influence on the strength of the polar branch of the residual circulation by means of the atmospheric wave activity.

1. Introduction

[2]   The thickness of the ozone layer above the Arctic in spring exhibits strong interannual variations. Only about half of this year-to-year variability is explained by the variability of wintertime chemical ozone loss [*Rex et al.*, 2004]. Apparently, the interannual variability of dynamical ozone supply is just as important [e.g., *Chipperfield and Jones*, 1999; *Andersen and Knudsen*, 2002; *Weber et al.*, 2003]. This motivates an increased interest in understanding the dynamical processes that are relevant for the supply of ozone to polar regions.

[3]   Over the winter months stratospheric air experiences diabatic descent within the polar vortex, which can vary with time and location. This vertical motion of air through the polar stratosphere is part of the residual mean circulation which shows significant year-to-year variability. The circulation transports air masses from tropical into midlatitude and polar regions. The overall process strongly influences the stratospheric distribution of trace gases and in particular the total abundance of ozone observed over the polar regions in late winter. The residual circulation is stronger and more variable in the Northern Hemisphere (NH) and leads to a pronounced dynamical variability in the Arctic compared to the Antarctic. To assess the impact of variability of the mean transport of mass with the residual circulation on the distributions of trace gases and particularly on the distribution of ozone in the Arctic polar vortex, it is important to study the interannual variability and the zonal structure of diabatic descent.

[4]   In principle there are two ways to derive the net winter polar descent from atmospheric data. First, observations of trace gases in the polar stratosphere can be used to estimate diabatic descent rates [e.g., *Schoeberl et al.*, 1992; *Manney et al.*, 1995; *Schoeberl et al.*, 1995; *Abrams et al.*, 1996; *Greenblatt et al.*, 2002; *Ray et al.*, 2002; *Jin et al.*, 2006]. This method is based on the observed descent of tracer isopleths measured during field campaigns or by satellite instruments and is restricted by the limited number of trace gas measurements that are available during polar night. Second, diabatic descent rates can be quantified by using calculated diabatic heating rates from radiative transfer models [*Rosenfield et al.*, 1994; *Manney et al.*, 1994; *Rosenfield and Schoeberl*, 2001]. These studies are based on the fact that diabatic motion in the stratosphere is determined by radiative processes. They use temperature fields from meteorological assimilation models to calculate the heating rates. Results from these studies are currently only available for a few winters during the 1990s, e.g., 1992–

[1]Alfred Wegener Institute for Polar and Marine Research, Potsdam, Germany.
[2]Now at Environment Canada, Toronto, Ontario, Canada.
[3]Now at IFM-GEOMAR, Kiel, Germany.

1993 [*Manney et al.*, 1994] and 1992–2000 [*Rosenfield and Schoeberl*, 2001].

[5] In this study we present the first long-term climatology of diabatic descent, averaged over the polar vortex, for the Arctic winters 1957/1958–2003/2004. The climatology is based on diabatic heating rate calculations coupled with trajectory calculations performed in the polar stratosphere during the NH winters. In addition to the overall vortex-averaged diabatic descent the spatial structure of the descent is analyzed for two different Arctic winters.

2. Method and Model

[6] Diabatic descent can be calculated by a time integration of descent rates on fixed grid points, i.e., in an Eulerian sense. However, the net vertical flux of mass is only correctly represented by Lagrangian calculations, that follow the air masses and include the interaction between horizontal and vertical motion of air. Therefore we use a trajectory model to calculate the three-dimensional (3-D) picture of diabatic descent during NH winters.

[7] In the trajectory model, air parcels are advected along isentropic surfaces using horizontal wind fields from meteorological assimilations. The vertical motion of parcels across isentropic surfaces is generated by diabatic heating rates. This approach avoids using vertical velocities from meteorological assimilations, which are too large [e.g., *Schoeberl et al.*, 2003; *van Noije et al.*, 2004; *Uppala et al.*, 2005] and far too noisy [*Schoeberl et al.*, 2003; *Wohltmann and Rex*, 2008] and therefore results in a more realistic vertical transport as originally shown by *Weaver et al.* [1993]. In the stratosphere it is possible to drive the diabatic vertical motions of trajectories with heating rates since the stratospheric diabatic motion within the residual circulation is determined by radiative processes. The approach based on diabatic heating rates has been successfully used in the polar stratosphere [*Konopka et al.*, 2004; *Chipperfield*, 2006], in the tropical lower stratosphere [*Schoeberl et al.*, 2003] and in the tropical tropopause layer (TTL) [*Konopka et al.*, 2007; *Immler et al.*, 2007; *Krüger et al.*, 2008]. The heating rates are computed off-line with the European Centre for Medium-Range Weather Forecasts (ECMWF) radiative transfer model which is described in section 2.1. The trajectory model is introduced in section 2.2.

[8] A method is developed to quantify the vortex-averaged diabatic descent during the NH winter from the trajectory runs. Furthermore, the diabatic descent is calculated as a function of equivalent latitude and potential temperature. We link the interannual variability of diabatic descent with variability of temperature anomalies and Eliassen-Palm (EP)-flux anomalies based on the multilinear regression technique. All the methods are described in section 2.3. The differences between Eulerian and Lagrangian calculations are presented in section 2.4. Results from calculations based on diabatic heating rates are compared with results from equivalent calculations based on vertical winds in section 2.5.

2.1. Radiation Transfer Model

[9] Radiative transfer calculations are performed every 6 hours for a $2.5° \times 2.5°$ latitude-longitude grid on 23 standard pressure levels with a stand alone version of the ECMWF radiative transfer model [*Morcrette et al.*, 1998]. The longwave computations are based on the Rapid Radiation Transfer Model (RRTM) [*Mlawer et al.*, 1997] which provides a reasonable balance between precision and computational efficiency. The RRTM uses the correlated-k method whereas the k-distributions are attained directly from the Atmospheric and Environmental Research, Inc. (AER) line-by-line model. The shortwave part of the radiation scheme is based on the photon path distribution method which was originally developed by *Fouquart and Bonnel* [1980]. To perform the spectral integration the solar spectrum is divided into 4 subintervals between 0.2 and 4 μm.

[10] Input data for temperatures and cloud properties are obtained from the ECMWF reanalysis (ERA40) [*Uppala et al.*, 2005] and after December 1999 from the ECMWF operational analysis (opECMWF) [*Simmons et al.*, 2005]. For some years there is an unrealistic oscillatory temperature structure in the vertical with an amplitude of a few degrees in the Arctic stratosphere [*Uppala et al.*, 2005; *Manney et al.*, 2005; *Gobiet et al.*, 2005]. We compare temperature fields from ECMWF with those from the Free University of Berlin (FUB) analysis and the National Center for Environmental Prediction Reanalysis data set (NCEP-REA). Although the NCEP-REA temperature fields are biased and have there deficiencies [e.g., *Manney et al.*, 2005] they are suitable to detect the time periods during which the oscillatory temperature structures in the two ECMWF analysis are particularly pronounced. The artificial temperature fluctuations are quite sporadic and tend to appear during cold barotropic conditions. They are most pronounced during only a few periods in individual years and are stronger at upper stratospheric levels. On the basis of the comparison between ECMWF, FUB and NCEP-REA data we identify the levels and periods when these fluctuations are particularly strong. We flag these regions and limit the interpretation of our analysis to periods that are not significantly influenced by these temperature fluctuations. A region is flagged if the deviation between the temperature profile from FUB or NCEP-REA and from ECMWF shows oscillations stronger than 10 K at the grid point 80°N, 10°E for more than 3 days. The center of the polar vortex is directly placed over the European Arctic in a long-term climatology [e.g., *Labitzke*, 1999]. Therefore the grid point 80°N, 10°E is appropriate to present the evolution of the stratospheric temperatures within the polar vortex. Close inspection of the temperature structures shows that they are always fairly large-scale and the conditions at this grid point represent the overall strength of the oscillations. With this algorithm the ERA40 winters from 1957/1958 until 1998/1999 and the opECMWF winters from 1999/2000 until 2003/2004 are examined. As a result January 1990, December 1995 and the first half of December 1996, are flagged above 550 K.

[11] The species treated in the radiative transfer model are water vapor, ozone, carbon dioxide, methane, nitrous oxide and the common halocarbons. The long-lived species are assumed to be well mixed and are set to standard mixing ratios for greenhouse gases. The CO_2 trend is prescribed. Ozone data are derived from the TOMS/GOME based CATO climatology [*Brunner et al.*, 2006] which is given

in an equivalent latitude - potential temperature reference frame. Water vapor is taken from the SAGE II climatology [*Chiou et al.*, 1997].

2.2. Trajectory Calculations

[12] The diabatic trajectory calculations are carried out in isentropic coordinates using horizontal winds from ERA40 and after December 1999 from opECMWF to advect air parcels along isentropic surfaces and using off-line calculated heating rates to generate the vertical motion. The numerical integration is performed with the implicit trapezoidal rule consistent for all three dimensions. Comprehensive tests show that this approach is more efficient and at least as precise as trajectory calculations with the explicit classical fourth-order Runge–Kutta method [*Tegtmeier*, 2007]. South of 85°N the integration step is carried out in Cartesian coordinates, while poleward of this latitude spherical geometry is used. The ERA40/opECMWF winds and the heating rates are taken on a 2.5° × 2.5° grid on 23/21 pressure levels between 1000 and 1 hPa. Winds and heating rates at the air parcel positions are calculated by linear interpolation in the horizontal and linear interpolation in log(p) in the vertical. The data fields are given for every 6 hours and are linearly interpolated in time to the trajectory time step of 20 min.

[13] To examine the origin of lower stratospheric air in late winter 3-D backward trajectory calculations are carried out within the Arctic stratosphere for a 3 month period. Approximately 51000 air parcels are initialized on 16 equally spaced isentropes between $\Theta = 400$ and 550 K covering the lower stratosphere. On each isentrope 3200 starting points are given on a grid with an equidistant spacing between 50°N and 90°N. The starting date is 10 March of the respective winter and the trajectories are calculated backward in time until 1 December of the same winter.

2.3. Diabatic Descent

[14] The trajectory calculations give a complex 3-D picture of the motion of stratospheric air masses during Arctic winter. For the time span of 3.5 months the accuracy of an individual trajectory is uncertain mainly due to errors in the meteorological wind fields [*Schoeberl et al.*, 2003]. However, by taking a statistical approach the properties of the trajectories can be used to derive information about the mean transport of air. We are particularly interested in the Lagrangian diabatic descent within the polar vortex. Hence we calculate the mean change of the potential temperature for all trajectories inside the polar vortex from the beginning of winter until spring.

[15] The location of the vortex can be determined based on the Rossby-Ertel potential vorticity PV. The edge of the vortex is defined based on the criterion from *Nash et al.* [1996], i.e., based on the meridional gradient of PV versus equivalent latitude ϕ_e and on the wind speed constraint. Equivalent latitude of a PV contour is defined as the latitude that encloses an area as large as the area enclosed by the PV contour [*Butchart and Remsberg*, 1986]. PV fields are taken from the ECMWF data sets. Our method is restricted to time periods and regions where the polar vortex exists and its edge is well defined. To not contaminate our results by the effects of the final warming we have chosen the start day of the trajectories quite early in winter.

[16] Well known problems with noise in the wind data from meteorological assimilation models [e.g., *Schoeberl et al.*, 2003] result in excessive flux of trajectories across the vortex edge. We want to analyze the vortex-averaged descent independently of this exaggerated exchange across the vortex edge. Therefore we divide the winter into time intervals of 14 days which are short enough to ensure that the artificial flux across the vortex edge is minimal. On the other hand the intervals are chosen long enough so that the trajectories have enough time to circle around the polar vortex at least once during each time interval. The diabatic descent is averaged along the path of the air parcel within the polar vortex for the 14 day long periods and the Lagrangian concept is preserved. For each time interval we determine all the trajectories which stay inside the polar vortex and average the descent of all these trajectories to estimate the Lagrangian diabatic descent. Also, we just use the trajectories which are within certain 10 K wide Θ - intervals at the beginning of each time interval and hence the Lagrangian diabatic descent will be estimated as function of time and altitude. With this method it is possible to derive the 2-D vortex-averaged descent from the complex 3-D trajectory information.

[17] We also analyze the spatial structure of the descent, i.e., the descent rates as a function of equivalent latitude, time and potential temperature. To do so, we average the change of potential temperature along the trajectories within certain Θ - ϕ_e - intervals for the individual time intervals of 14 days. Finally, we can obtain the Lagrangian diabatic descent by integrating the descent rates over the winter. The integration is carried out on levels of constant spring equivalent potential temperature Θ_e - the potential temperature an air mass reaches in spring [*Rex et al.*, 2004].

[18] We link the interannual variability of diabatic descent with variability of temperature anomalies. Therefore we look at the monthly mean north pole temperatures at 30 hPa for December, January and February from the radiosonde analysis of FUB. We use these three time series as explanatory variables to calculate a fit of the diabatic descent with the multilinear regression. The approach used here in the multilinear regression technique is the least squares minimization. This will lead to those three coefficients for the linear combination of the three temperature time series which will produce an optimal fit of the diabatic descent (giving the best correlation between fit and descent). In an analogous manner we link the interannual variability of diabatic descent with variability of EP-flux anomalies. Therefore we use three monthly mean time series of the vertical component of the EP-flux through 100 hPa, averaged between 45°N and 75°N, for December, January and February from ERA40/opECMWF. The EP-flux is calculated according to equations 3.5.3 a and b of *Andrews et al.* [1987]. Again we calculate a fit of the diabatic descent based on the three EP-flux time series as explanatory variables with the multilinear regression technique.

2.4. Comparison of Lagrangian and Eulerian Approach

[19] Results from our calculations based on the Lagrangian approach are compared with results from equivalent calculations in an Eulerian sense. For the latter approach we
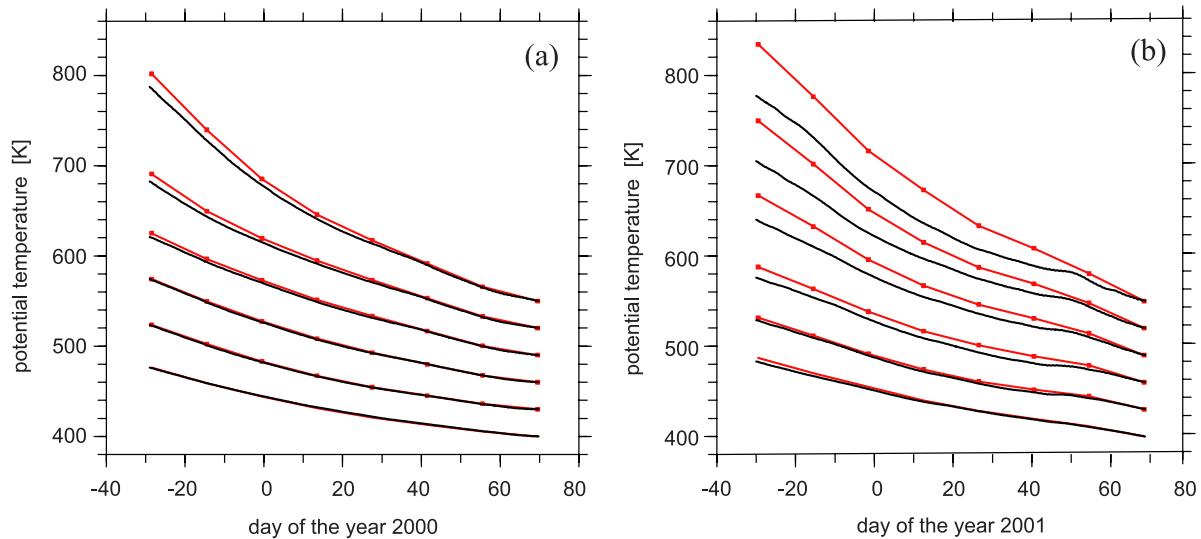
Figure 1. Vortex-averaged diabatic descent in the form of the time evolution of potential temperature during the winter based on the Lagrangian approach (red) and the Eulerian approach (black). The vortex-averaged descent is shown for six starting levels for winters (a) 1999/2000 and (b) 2000/2001.

average the diabatic descent rates derived from radiative transfer calculations over the polar vortex for each 6 hour time step and each of 51 equally spaced isentropes between 400 K and 900 K. This method produces vortex-averaged Eulerian descent rates as a function of potential temperature and time. We integrate the descent rates from 1 December until 10 March to obtain the Eulerian diabatic descent for the 3.5 months long time period. Figure 1 shows the vortex-averaged diabatic descent based on the two approaches for the cold Arctic winter 1999/2000 [*Manney and Sabutis*, 2000] and the warm Arctic winter 2000/2001 [*Manney et al.*, 2005]. The vortex-averaged descent calculated with the Eulerian approach is weaker than the Lagrangian descent. These differences are more pronounced for the winter 2000/2001 where they can be up to 25%. The differences are caused by correlations between temperature anomalies and horizontal wind anomalies along trajectories. Because of such systematic correlations individual air masses encounter temperature anomalies (and corresponding anomalies in radiative heating or cooling rates) for shorter or longer periods of time, than one would think just based on a snapshot of the temperature (or heating/cooling) field. The variations in horizontal velocities are not taken into account if the heating/cooling field is just integrated in an Eulerian manner. Since these correlations are particularly pronounced for winters with strong wave activity we expect to find larger differences between the two approaches for the more disturbed and dynamically active winters. This is confirmed by our results showing strong differences for the disturbed winter 2000/2001 and a good agreement between the two approaches for the cold and undisturbed winter 1999/2000. Since the two approaches can give different results it is necessary to use the Lagrangian approach to estimate the vertical mean mass transport accurately.

2.5. Comparison of Diabatic and Kinematic Approach

[20] The vertical motion of the trajectories can be calculated with heating rates (diabatic trajectories) or with the vertical velocities (kinematic trajectories). Vertical velocities are hard to measure. A simple way to derive vertical wind fields is via the divergence of horizontal winds in the meteorological assimilations. Because the vertical velocities are by a factor of 100 smaller than the horizontal velocities, this approach can produce noisy data. Indeed the vertical velocities within the ECMWF data sets tend to be too noisy and they drive a mean mass transport that is too fast [*van Noije et al.*, 2004; *Uppala et al.*, 2005]. We want to assess whether this is in particular true in the polar wintertime stratosphere.

[21] Figure 2 shows the time evolution of the potential temperature of all the trajectories inside the polar vortex from 10 February 2002 until 10 March 2002. We resample the trajectories after a 14 day long time period to be within a 10 K wide Θ - interval around the new vortex-averaged potential temperature. Therefore the vertical spread of the trajectories shown in Figure 2 collapses after 14 days and then increases thereafter. Comparing the kinematic (Figure 2a) and the diabatic trajectories (Figure 2b) reveals that the vertical velocities are much noisier than the heating rates since trajectories driven by these vertical velocities display a stronger vertical dispersion. From calculating the corresponding heating rates for the kinematic vertical velocities and from comparisons with vertical eddy diffusion coefficients that have been derived from observations [*Wohltmann and Rex*, 2008] we know that the dispersion of the kinematic trajectories is unrealistic and that the kinematic vertical velocities are much too noisy. Furthermore, Figure 2 shows the vortex-averaged diabatic descent in the form of the thick lines. The diabatic trajectories show a descent of 38.6 K for 4 weeks while the kinematic trajectories display a descent of 209.5 K for the same time period. We know from measured tracer distributions [e.g., *Schoeberl et al.*, 1992; *Manney et al.*, 1995; *Greenblatt et al.*, 2002] and from other model studies [*Rosenfield et al.*, 1994] that diabatic velocities of the order of 1 K/day are realistic, whereas the order of magnitude of the kinematic
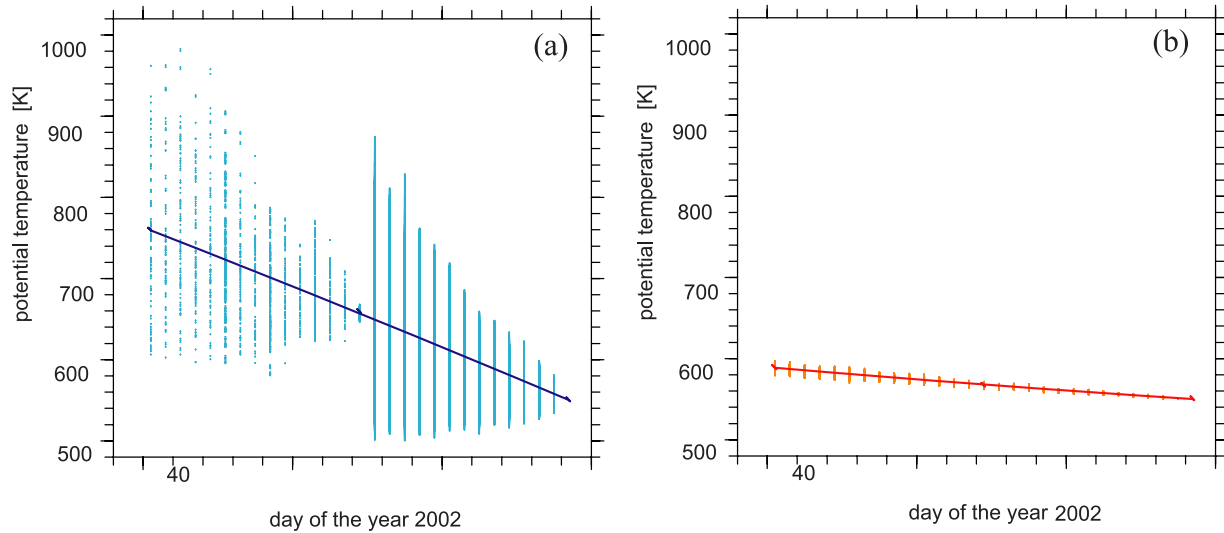
Figure 2. Time series of the potential temperature of all the (a) kinematic and (b) diabatic trajectories inside the polar vortex from 10 February 2002 until 10 March 2002. The thin lines represent the vertical spread of the potential temperature once per day. The vortex-averaged Lagrangian descent is shown as a thick line for both approaches.

value is much too big. The comparison shows that the kinematic approach results in an excessive vertical transport in the polar stratosphere and therefore we use the diabatic approach throughout this study. A detailed validation of the diabatic approach follows in section 3.2. Our conclusions regarding the two approaches for the polar stratosphere are in agreement with results from transport studies in the tropical stratosphere from *Schoeberl et al.* [2003] and in the TTL from *Immler et al.* [2007] and *Krüger et al.* [2008]. These two latter companion studies demonstrated the great advantage of using our diabatic trajectories instead of

kinematic trajectories for simulating tropical cirrus clouds and investigating transport processes in the TTL.

3. Evaluation of the Approach

[22] To validate the diabatic heating rates we compare our results from the radiative transfer calculations with results from the Fu-Liou radiation scheme [*Fu and Liou*, 1993], which is a detailed and complex radiative transfer model. Furthermore, we compare the vortex-averaged descent derived from the diabatic trajectory analysis with
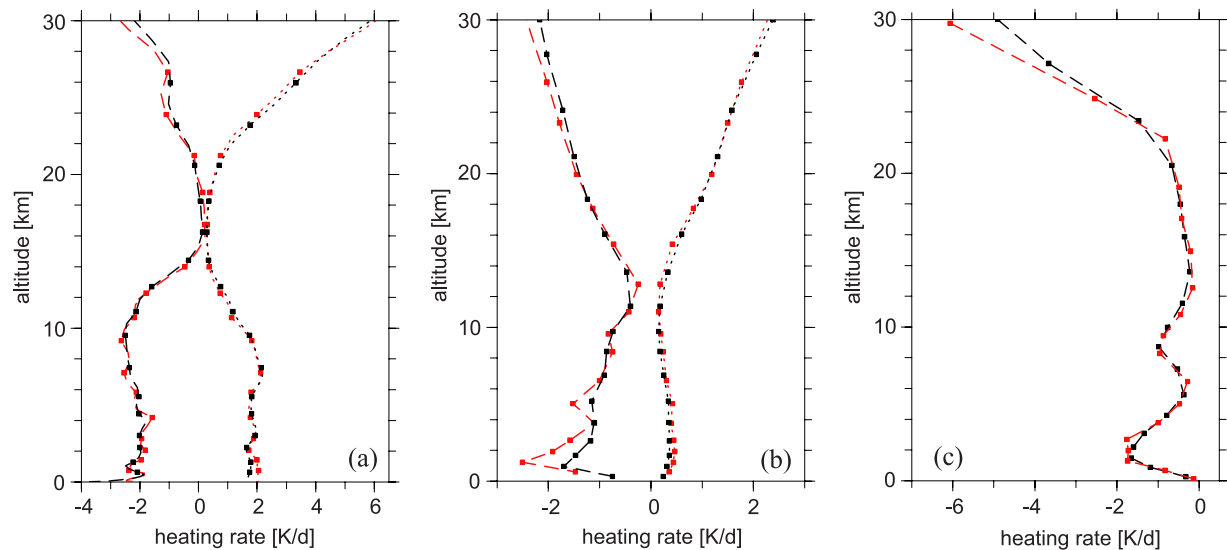
Figure 3. Profiles of the longwave (dashed) and shortwave (dotted) heating rates calculated with the ECMWF radiation scheme (red) and the Fu-Liou radiation scheme (black). (a) Heating rates at 0°N, 90°W for 16 March 1992, 18:00 UTC; (b) heating rates at 80°N, 90°W for 16 March 1992, 18:00 UTC; and (c) heating rates at 87.5°N, 90°W for 16 January 1992, 18:00 UTC.
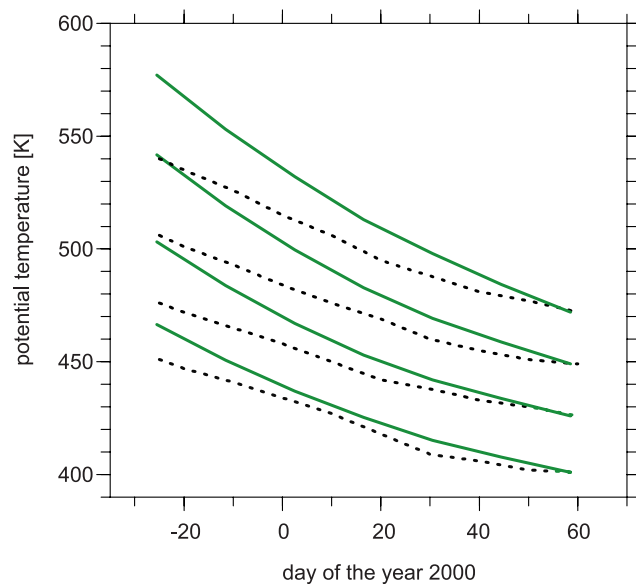
Figure 4. Lagrangian diabatic descent based on N_2O measurements in the polar vortex from *Greenblatt et al.* [2002] (black dotted line) and based on our vortex averaging model calculations (green drawn-through line) for four starting isentropes from 5 December 1999 until 28 February 2000.

measured tracer distributions and results from other model studies.

3.1. Validation of the Radiative Transfer Calculations

[23] A detailed intercomparison case study between heating rates calculated with the ECMWF radiation scheme and the Fu-Liou radiation scheme was carried out to validate the radiative transfer calculations [*Tegtmeier*, 2007]. The comparison was done for very constrained conditions, i.e., for exactly the same input data for both models.

[24] Figure 3 displays three examples of the comparison. The first example (Figure 3a) is a case study carried out over Galapagos, 0°N, 90°W for 16 March 1992 corresponding to the location and time of a radiation balance study from *Gettelman et al.* [2004]. The tropical heating rates from the ECMWF radiation scheme and the Fu-Liou radiation scheme show a very good agreement with differences less than 0.1 K at the level of zero net heating (∼18 km altitude). The second example is an intercomparison at polar latitudes, i.e., heating rates at 80°N, 90°W for 16 March 1992 (Figure 3b), which demonstrate a very good agreement in the longwave and in the shortwave region with differences of less than 0.2 K/day in the middle and lower stratosphere. The last example displays a comparison at the grid point 87.5°N, 90°W, for 16 January 1992 (Figure 3c) and therefore only longwave heating rates are given. Except for some deviations above 28 km we find again a very good agreement. Since the Fu-Liou radiative transfer model is a detailed and complex radiation model we can use the good agreement between the two models as a validation of our own radiative transfer calculations.

3.2. Validation of Diabatic Descent

[25] We compare our estimates of the vortex-averaged descent based on diabatic trajectories with estimates of the

diabatic descent based on measured tracer distributions from satellite data and Arctic field campaigns. Figure 4 displays the descent derived from the measurements of the long-lived trace gas N_2O in winter 1999/2000 [*Greenblatt et al.*, 2002] (black dotted line). Figure 4 also includes the vortex-averaged descent from our model calculations for the corresponding time period and starting isentropes (green line). The comparison shows differences between the measurements and our model results which are large at higher altitudes and vary between 27% and 42%. These differences can be due to a number of reasons. First the studies based on measured tracer distributions do not take into account the effect of mixing across the vortex edge. Therefore the analysis of the trace gas profiles can underestimate the real vortex-averaged descent. Also, the differences can be caused by the fact that the tracer distributions are based on local measurements within the polar vortex and our estimated descent is calculated as a vortex average. In general, uncertainties in the quality of the stratospheric temperature and wind fields can lead to uncertainties in our model results. Further comparison with a study from *Ray et al.* [2002] based on the SAGE III ozone loss and validation experiment (SOLVE) shows better agreement with differences varying between 7% and 30% for air masses between 700 K and 550 K at the beginning of winter. The vertical profiles of the diabatic descent within the polar vortex for the winter 1999/2000 from *Ray et al.* [2002] were estimated while taking effects of mixing across the vortex edge into account.

[26] A simulation with the Chemical Lagrangian Model of the Stratosphere (CLaMS), which uses cross-isentropic velocities calculated with a radiation module, provides estimates of the mean diabatic descent within the vortex [*Konopka et al.*, 2004]. The diabatic descent derived with CLaMS and our estimated diabatic descent are in reasonable agreement with differences between 13% and 22% for air masses between 550 K and 700 K at the beginning of winter. Model studies from *Rosenfield and Schoeberl* [2001] investigate transport processes in the polar vortex with the help of comprehensive diabatic trajectory runs for the time period 1992–2000. They find a diabatic descent of 40–50 K for January and February 1995/1996 for the region between 460 K and 510 K. Our model calculations give a vortex-averaged descent of 57 K for the same time period and altitude. The trajectories in the study from *Rosenfield and Schoeberl* [2001] experience between 13% and 29% less diabatic descent which is in reasonable agreement with our results.

[27] Further detailed sensitivity studies were carried out by *Tegtmeier* [2007]. The most important results are that the quality of the temperature fields has a strong influence on the Lagrangian diabatic descent, whereas the influence of ozone fields, water vapor and cloud resolution ranges from small to negligible. The study points out that variations of the time step or the number of trajectories have only a small influence on the results.

4. Case Studies

[28] Case studies for two different winters are used to investigate the influence of the different meteorological conditions in the NH stratosphere on the diabatic descent.
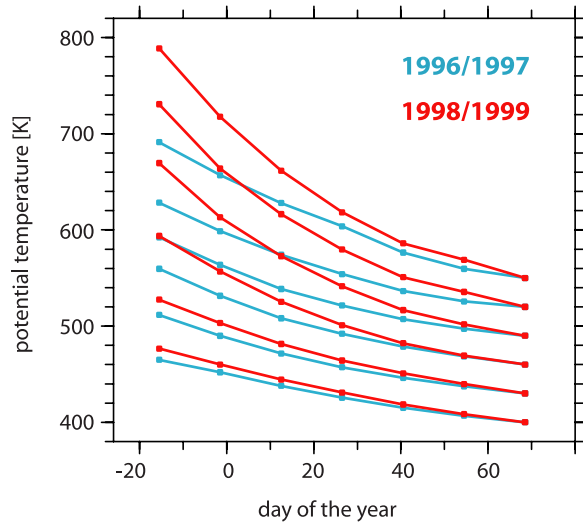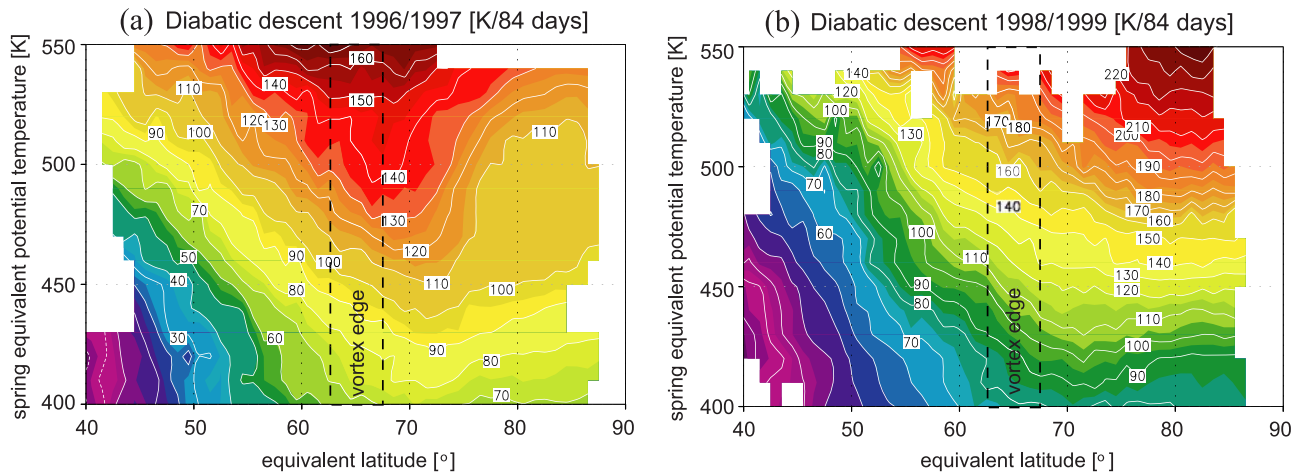
Figure 5. Vortex-averaged diabatic descent for six starting levels for the time period from 15 December until 10 March for the two winters 1996/1997 (blue lines) and 1998/1999 (red lines).

The 1996/1997 winter became cold at the beginning of January and had a strong and stable polar vortex with a late final warming at the end of April [*Naujokat and Pawson*, 1998]. The 1998/1999 winter was characterized by a weaker vortex and by much stronger wave activity apparent in two major midwinter warmings which occurred in December and February [*Naujokat et al.*, 2002].

[29] Figure 5 shows the Lagrangian vortex-averaged diabatic descent in the form of time evolution of the potential temperature for the 1996/1997 winter (blue lines). To avoid the flagged regions with temperature oscillations, the time period is limited to the 12 weeks between 15 December and 10 March. The vortex-averaged descent depends on the altitude: the lowest-level experiences a vortex-averaged descent of 65 K for the shown winter period (84 days) whereas the upper level descends over twice as much

(140 K). Figure 5 also displays the corresponding results for the winter 1998/1999 (red lines). Here the descent is three times stronger for the upper levels than for the lower levels (250 K/84 days vs. 80 K/84 days). The descent rates depend on time, with a more intensive descent in early winter compared to late winter. The time dependence results from the annual cycle of the deviation from the radiative equilibrium temperature and is especially strong for higher levels. The dependence of the descent on altitude and time is consistent with previous studies [e.g., *Manney et al.*, 1994; *Rosenfield and Schoeberl*, 2001]. A direct comparison of the results for the two winters demonstrates clearly that the descent is much weaker in winter 1996/1997 than two years later. In general a warm winter with more extratropical wave driving leads to a stronger meridional component of the residual circulation and therefore to stronger adiabatic compression and heating in the polar vortex region. This results in larger deviations from the radiative equilibrium temperature and stronger radiative cooling (diabatic descent) during the polar winter [*Holton et al.*, 1995]. The understanding of these dynamical processes is reflected in our results which show stronger diabatic descent during the warm and dynamically active winter 1998/1999.

[30] Figure 6 displays the diabatic descent as function of equivalent latitude and spring potential temperature for the two winters. Again the time period is constrained to the 12 weeks between 15 December and 10 March. The dashed lines show the approximate positions of the edge of the polar vortex throughout the winter. In both winters the magnitude of diabatic descent grows with increasing Θ_e, which is consistent with our findings for the vortex-averaged descent and results from previous studies [e.g., *Manney et al.*, 1994]. The absolute values are much higher for the warm and disturbed winter 1998/1999 (Figure 6b) than for the colder winter 1996/1997 (Figure 6a) in all regions of the polar vortex (note the different color scales). Furthermore, there are pronounced differences in the zonal structure of the diabatic descent. During the cold and stable polar winter 1996/1997 the strongest diabatic descent along

Figure 6. The Lagrangian descent (K/84 days) as a function of equivalent latitude and spring equivalent potential temperature for the time period from 15 December until 10 March for (a) winters 1996/1997 and (b) 1998/1999.
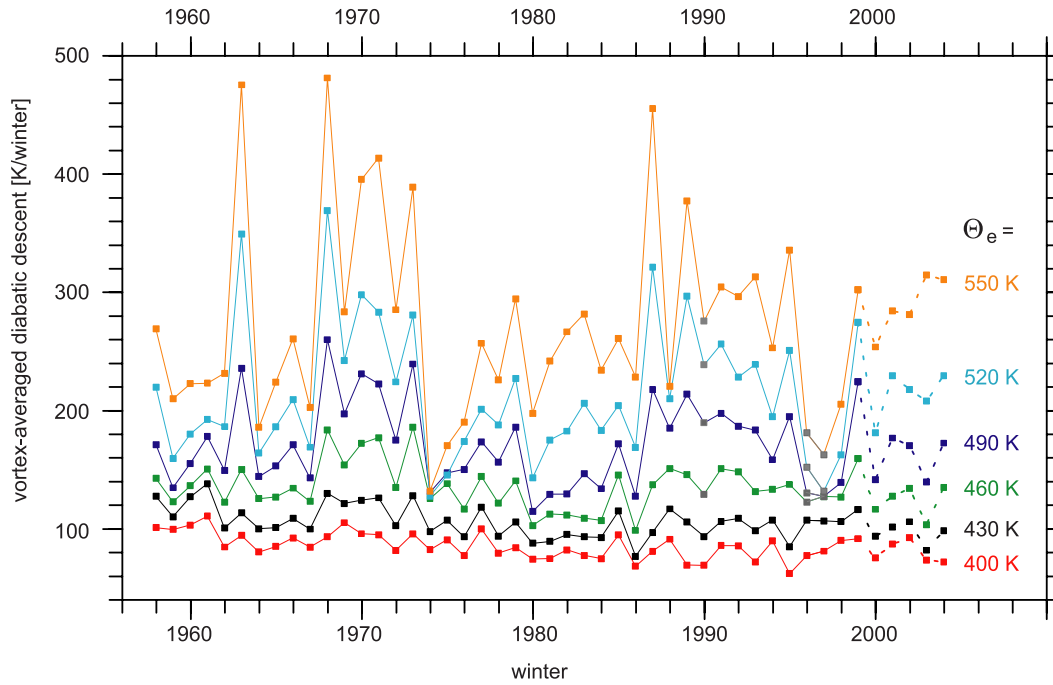
Figure 7. Time series of the vortex-averaged diabatic descent for six chosen starting isentropes for 47 winters from 1957/1958 until 2003/2004. The first 42 winters are based on ERA40 (solid line) and the last five winters are based on the opECMWF data (dashed line). The results for the three winters which are flagged because of unrealistic vertical temperature oscillations are marked with gray dots.

one level of equal Θ_e is close to the vortex edge, whereas in the disturbed winter 1998/1999 we find the strongest descent in the vortex core. Previous work from *Schoeberl et al.* [1992] has shown that for the Antarctic polar vortex of the winter 1987 the strongest descent is close to the vortex edge. *Manney et al.* [1994] examined the Antarctic polar vortices of 1992 and 1993 and the Arctic polar vortices of 1992/1993 and 1993/1994 and found that descent was stronger near the vortex edge in late winter. A Chemistry Transport Model study for a cold winter/spring period from *Lemmen et al.* [2006] derived differential diabatic descent in the Arctic stratosphere with the strongest descent occurring around $\phi_e = 60°N$. All these results are in good agreement with our findings for the winter 1996/1997, which was unusually cold and quiescent in late winter [*Pawson and Naujokat*, 1999]. The zonal structure of diabatic descent in the cold winter 1996/1997 is very similar to the structure of diabatic descent during the Antarctic winters examined by *Manney et al.* [1994] and *Schoeberl et al.* [1992]. However, *Manney et al.* [1994] found that in early winter diabatic descent was strongest near the vortex core in more quiescent years, and near the vortex edge when wave activity was strong. This is different from our results which show maximum descent in the vortex core for the warmer and more disturbed winter 1998/1999. Interpreting our findings about the zonal structure of the diabatic descent for the two winters leads us to the following conclusions. During a disturbed winter with intensive wave activity it is very likely that atmospheric waves can penetrate deeper into the polar vortex and therefore lead to strong descent in the vortex core region. During a cold and undisturbed winter with less wave activity the center of the wave breaking and

therefore of the diabatic descent is probably the vortex edge region rather than the vortex core.

5. Interannual Variability

[31] We compile a multiyear time series of the vortex-averaged diabatic descent for 47 winters from 1957/1958 until 2003/2004 to investigate the interannual variability during NH winter. The climatology gives a detailed picture of the intensity and altitude dependence of the stratospheric vertical transport processes during Arctic winter. Figure 7 displays the time series of the vortex-averaged diabatic descent for 6 starting isentropes. The results for the three winters which are flagged because of unrealistic vertical temperature oscillations are marked with gray dots. The first 42 winters are based on ERA40 (solid line) and the last five winters are based on the opECMWF data (dashed line). For the three winters 1999/2000, 2000/2001 and 2001/2002 both data sets are available. The vortex-averaged descent (and the zonal structure of the descent) calculated for the overlapping period with ERA40 and with opECMWF data show a very good agreement for the time periods where no unrealistic vertical temperature oscillations occur [*Tegtmeier*, 2007]. Therefore it is justified to extend the time series based on ERA40 with results based on opECMWF data. To avoid the vertical temperature oscillations which occur occasionally in ERA40 for the three winters 1999/2000, 2000/2001 and 2001/2002 the opECMWF data is used for these winters throughout. The complete time series of the vortex-averaged diabatic descent shows very pronounced interannual variability which expresses the year-to-year variability of the polar branch of the residual circulation and is especially strong for higher
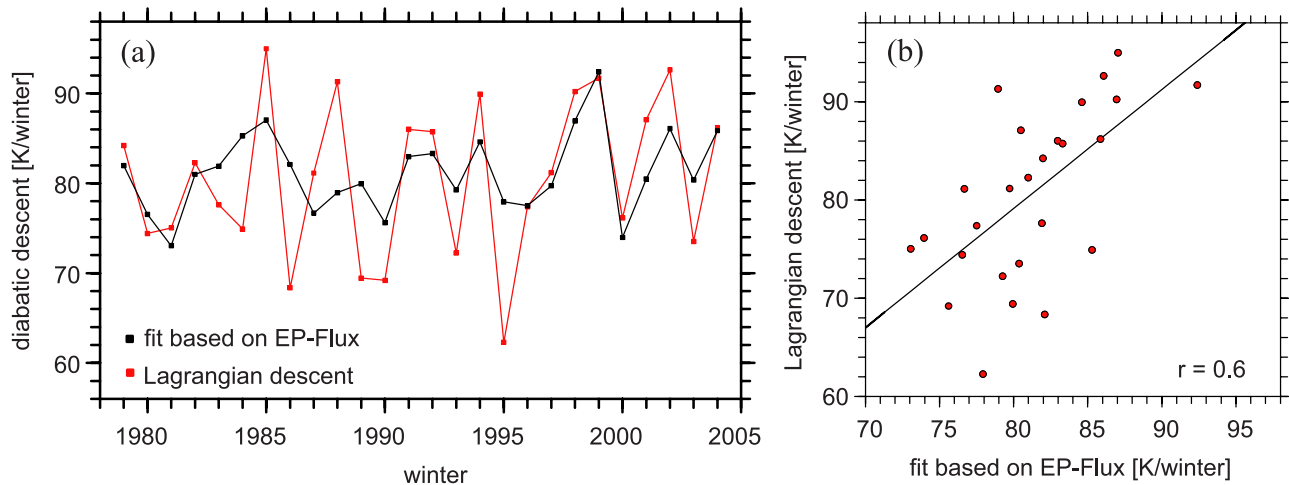
Figure 8. (a) Time series starting at 1979 of the diabatic descent for the starting isentrope $\Theta_e = 400$ K (red) and the corresponding fit based on the EP-flux (black). (b) Scatterplot of diabatic descent and EP-flux-based fit.

isentropes. Because of this high interannual variability, trend estimates suffer from large uncertainties and hence we avoid any trend discussion based on this climatology. We focus on analyzing the interannual variations of the diabatic descent and relate them to the variability of temperature anomalies and EP-flux anomalies.

[32] The fit of the diabatic descent based on the independent and reliable temperature time series of FUB [*Randel et al.*, 2003] is highly correlated with our calculated diabatic descent: for the start isentrope $\Theta_e = 400$ K the correlation coefficient is 0.77 for the whole time series from 1957/1958 until 2003/2004 and 0.81 for the shorter time series starting at 1979/1980. Both correlation coefficients are statistically significant at the 99% confidence level. The high correlation demonstrates the direct connection between temperature anomalies and diabatic descent, as expected.

[33] Temperature anomalies are driven by atmospheric wave activity which is illustrated by the strong correlation between polar temperatures and the vertical component of EP-flux [*Newman et al.*, 2001]. Given the uncertainties of vertical wind velocities from assimilation systems, it is for the first time possible to link not only EP-flux and temperature anomalies but also EP-flux and diabatic descent.

[34] Figure 8a displays the time series starting at 1979/1980 of our calculated diabatic descent for the starting isentrope $\Theta_e = 400$ K (red) and the corresponding fit based on the three monthly time series of EP-flux in December, January and February (black). Figure 8b shows the same data in form of a scatterplot. The correlation coefficient between the diabatic descent and the fit is 0.6. Correlation coefficients greater than 0.42 are statistically significant at the 95% confidence level for the 23-year time series. The three regression coefficients used to calculate the fit describe the weighting of the three monthly EP-flux time series. The coefficient for the EP-flux in December is three times as large as the coefficients for EP-flux in January or February, illustrating that there is a stronger correlation between diabatic descent and EP-flux in December than there is in January or February. This is consistent with the results from *Newman et al.* [2001] who found the strongest

correlations between EP-flux and temperature in winter for a time lag of 1-2 months. The correlation between EP-flux fit and diabatic descent is less pronounced than the correlation between temperature fit and diabatic descent which reflects the fact that the wave activity first drives the temperature anomalies which then cause the diabatic descent. The vertical component of extratropical EP flux at 100 hPa (lowermost stratosphere) is a measure of the vertical flux of zonal momentum of tropospheric waves which have entered the stratosphere. The correlation between EP-flux and descent shows that a large fraction of the interannual variability of the strength of the descending branch of the residual circulation is driven by variability in tropospheric dynamics. This is consistent with our theoretical understanding of the mechanisms that drive the residual circulation.

6. Conclusions

[35] Multiyear calculations of Lagrangian diabatic descent based on isentropic trajectories and radiative heating rates have been carried out in order to investigate the mean mass transport of air in the Arctic wintertime stratosphere. Diabatic descent can also be calculated by a time integration of descent rates on fixed grid points, i.e., in an Eulerian sense. However, the vertical mean mass transport is more accurately represented by Lagrangian calculations, that follow the air masses and include the interaction between horizontal and vertical motion of air. The Eulerian and Lagrangian approach give different results which are particularly pronounced for winters with strong wave activity.

[36] Investigating the influence of different vertical velocities for a case study for the winter 2001/2002 demonstrates that trajectories based on diabatic heating rates result in a much more realistic vertical transport than trajectories based on vertical winds from ECMWF. Therefore in the polar stratosphere the diabatic approach provides a useful opportunity to overcome the known problems of noisy and biased vertical winds from meteorological assimilation systems. These results are consistent with previous studies.

[37] The overall vortex-averaged diabatic descent and the spatial structure of the descent have been analyzed for two different Arctic winters to investigate the influence of meteorological conditions. The comparison clearly shows more diabatic descent during a warm and dynamically active winter (1998/1999) than during a cold and undisturbed winter (1996/1997). Furthermore, the warm winter with strong wave activity is characterized by strong diabatic descent in the vortex core region, whereas during the colder undisturbed winter stronger diabatic descent is found at the vortex edge in good correspondence with Antarctic winter studies. This link between the meteorological conditions and the intensity and zonal structure of the diabatic descent is also found for other winters not shown here.

[38] We have compiled a multiyear time series of the vortex-averaged diabatic descent for 47 winters from 1957/1958 until 2003/2004. The climatology gives a detailed picture of the intensity and altitude dependence of the stratospheric vertical transport processes during Arctic winters. The vortex-averaged diabatic descent is characterized by a very pronounced interannual variability which expresses the year-to-year variability of the polar branch of the residual circulation. We have linked the interannual variability of diabatic descent with variability of temperature anomalies and EP-flux anomalies. The correlation between EP-flux and diabatic descent shows that tropospheric dynamics in the extratropics can have a strong influence on the polar branch of the residual circulation.

[39] Previous studies used diabatic descent rates from radiative transfer calculations to quantify the chemical ozone loss [e.g., *Konopka et al.*, 2004]. The vortex-averaged diabatic descent calculated here can be used to estimate the net dynamical supply of ozone caused by the net transport processes with the residual circulation [*Tegtmeier et al.*, 2008]. On the basis of this approach it is possible to quantify the relative importance of dynamical contributions due to mean transport of mass with the residual circulation and chemical contributions to Arctic wintertime ozone. The time series of the vortex-averaged descent can provide a useful diagnostic to validate net transport processes within the polar vortex in coupled Chemistry-Climate Models. Continuing the climatology for the most recent NH winters and for SH winters and comparing these results with descent rates based on measured tracer distributions can be investigated in a future study.

References

Abrams, M. C., et al. (1996), Trace gas transport in the Arctic vortex inferred from ATMOS ATLAS-2 observations during April 1993, *Geophys. Res. Lett.*, 23(17), 2345–2348.

Andersen, S. B., and B. M. Knudsen (2002), The influence of vortex ozone depletion on Arctic ozone trends, *Geophys. Res. Lett.*, 29(21), 2013, doi:10.1029/2001GL014595.

Andrews, D. G., J. Holton, and C. Leovy (1987), *Middle Atmosphere Dynamics*, Academic Press, London, U. K.

Brunner, D., J. Staehelin, H.-R. Künsch, and G. E. Bodeker (2006), A Kalman filter reconstruction of the vertical ozone distribution in an equivalent latitude–potential temperature framework from TOMS/GOME/SBUV total ozone observations, *J. Geophys. Res.*, 111, D12308, doi:10.1029/2005JD006279.

Butchart, N., and E. E. Remsberg (1986), The area of the stratospheric polar vortex as a diagnostic for tracer transport on an isentropic surface, *J. Atmos. Sci.*, 43, 1319–1339.

Chiou, E., M. McCormick, and W. Chu (1997), Global water vapor distributions in the stratosphere and upper troposphere derived from 5.5 years of SAGE II observations (1986–1991), *J. Geophys. Res.*, 102, 19,105–19,118.

Chipperfield, M. P. (2006), New version of the TOMCAT/SLIMCAT offline chemical transport model, *Q. J. R. Meteorol. Soc.*, 132, 1179–1203.

Chipperfield, M., and R. Jones (1999), Relative influences of atmospheric chemistry and transport on Arctic ozone trends, *Nature*, 400, 551–554.

Fouquart, Y., and B. Bonnel (1980), Computations of solar heating of the earth's atmosphere: A new parameterization, *Beitr. Phys. Atmos.*, 53, 35–62.

Fu, Q., and K. N. Liou (1993), Parameterization of the radiative properties of cirrus clouds, *J. Atmos. Sci.*, 50, 2008–2025.

Gettelman, A., P. M. F. Forster, M. Fujiwara, Q. Fu, H. Vomel, L. K. Gohar, C. Johanson, and M. Ammeraman (2004), The radiation balance of the tropical tropopause layer, *J. Geophys. Res.*, 109, D07103, doi:10.1029/2003JD004190.

Gobiet, A., U. Foelsche, A. Steiner, M. Borsche, G. Kirchengast, and J. Wickert (2005), Climatological validation of stratospheric temperatures in ECMWF operational analyses with CHAMP radio occultation data, *Geophys. Res. Lett.*, 32, L12806, doi:10.1029/2005GL022617.

Greenblatt, J. B., et al. (2002), Tracer-based determination of vortex descent in the 1999/2000 Arctic winter, *J. Geophys. Res.*, 107(D20), 8279, doi:10.1029/2001JD000937.

Holton, J. R., P. H. Haynes, M. E. McIntyre, A. R. Douglass, R. B. Rood, and L. Pfister (1995), Stratosphere–troposphere exchange, *Rev. Geophys.*, 33, 403–439.

Immler, F., K. Krüger, S. Tegtmeier, M. Fujiwara, P. Fortuin, G. Verver, and O. Schrems (2007), Cirrus clouds, humidity, and dehydration in the tropical tropopause layer observed at Paramaribo, Suriname (5.8°N, 55.2°W), *J. Geophys. Res.*, 112, D03209, doi:10.1029/2006JD007440.

Jin, J. J., et al. (2006), Severe Arctic ozone loss in the winter 2004/2005: Observations from ACE-FTS, *Geophys. Res. Lett.*, 33, L15801, doi:10.1029/2006GL026752.

Konopka, P., et al. (2004), Mixing and ozone loss in the 1999–2000 Arctic vortex: Simulations with the three-dimensional Chemical Lagrangian Model of the Stratosphere (CLaMS), *J. Geophys. Res.*, 109(D18), D02315, doi:10.1029/2003JD003792.

Konopka, P., et al. (2007), Contribution of mixing to upward transport across the tropical tropopause layer (TTL), *Atmos. Chem. Phys.*, 7, 3285–3308.

Krüger, K., S. Tegtmeier, and M. Rex (2008), Long-term climatology of air mass transport through the tropical tropopause layer (TTL) during NH winter, *Atmos. Chem. Phys.*, 8, 813–823.

Labitzke, K. G. (1999), *Die Stratosphäre*, Springer, Berlin.

Lemmen, C., R. Müller, P. Konopka, and M. Dameris (2006), Critique of the tracer-tracer correlation technique and its potential to analyze polar ozone loss in chemistry-climate models, *J. Geophys. Res.*, 111, D18307, doi:10.1029/2006JD007298.

Manney, G. L., and J. L. Sabutis (2000), Development of the polar vortex in the 1999–2000 Arctic winter stratosphere, *Geophys. Res. Lett.*, 27(17), 2589–2592.

Manney, G. L., W. R. Zurek, A. O'Neill, and R. Swinbank (1994), On the motion of air through the stratospheric polar vortex, *J. Atmos. Sci.*, 51, 2973–2994.

Manney, G., et al. (1995), Lagrangian transport calculations using UARS data. part I: Passive tracers, *J. Atmos. Sci.*, 52, 3049–3068.

Manney, G. L., K. Krüger, J. L. Sabutis, S. A. Sena, and S. Pawson (2005), The remarkable 2003–2004 winter and other recent warm winters in the Arctic stratosphere since the late 1990s, *J. Geophys. Res.*, 110, D04107, doi:10.1029/2004JD005367.

Mlawer, E. J., S. J. Taubman, P.D. Brown, M. J. Iacono, and S. A. Clough (1997), Radiative transfer for inhomogeneous atmospheres: RRTM, a validated correlated-k model for the longwave, *J. Geophys. Res.*, 102, 16,663–16,682.

Morcrette, J.-J., S. A. Clough, E. J. Mlawer, and M. J. Iacono (1998), Impact of a validated radiative transfer scheme, RRTM, on the ECMWF model climate and 10-day forecasts, *ECMWF Tech. Memo*, 47, 252.

Nash, E. R., P. A. Newman, J. E. Rosenfield, and M. R. Schoeberl (1996), An objective determination of the polar vortex using Ertel's potential vorticity, *J. Geophys. Res.*, 101/D5, 9471–9478.

Naujokat, B., and S. Pawson (1998), The unusual cold, persistent vortex in spring 1997, *BMBF Air Pollut. Res. Rep.*, 66, 50–53.

Naujokat, B., K. Krüger, K. Matthes, J. Hoffmann, M. Kunze, and K. Labitzke (2002), The early major warming in December 2001—Exceptional?, *Geophys. Res. Lett.*, *29*(21), 2023, doi:10.1029/2002GL015316.

Newman, P., E. Nash, and J. Rosenfield (2001), What controls the temperature of the Arctic stratosphere during the spring?, *J. Geophys. Res.*, *106*, 19,999–20,010.

Pawson, S., and B. Naujokat (1999), The cold winters of the middle 1990s in the northern lower stratosphere, *J. Geophys. Res.*, *104*, 14,209–14,222.

Randel, W., et al. (2003), The SPARC intercomparison of middle-atmosphere climatologies, *J. Clim.*, *17*, 986–1003.

Ray, E. A., F. L. Moore, J. W. Elkins, D. F. Hurst, P. A. Romashkin, G. S. Dutton, and D. W. Fahey (2002), Descent and mixing in the 1999–2000 northern polar vortex inferred from in situ tracer measurements, *J. Geophys. Res.*, *107*(D20), 8285, doi:10.1029/2001JD000961.

Rex, M., R. J. Salawitch, P. v. d. Gathen, N. R. P. Harris, M. P. Chipperfield, and B. Naujokat (2004), Arctic ozone loss and climate change, *Geophys. Res. Lett.*, *31*, L04116, doi:10.1029/2003GL018844.

Rosenfield, J. E., and M. R. Schoeberl (2001), On the origin of polar vortex air, *J. Geophys. Res.*, *106*, 33,485–33,497.

Rosenfield, J. E., P. A. Newman, and M. R. Schoeberl (1994), Computations of diabatic descent in the stratospheric polar vortex, *J. Geophys. Res.*, *99*, 16,677–16,689.

Schoeberl, M. R., L. R. Lait, P. A. Newman, and J. E. Rosenfield (1992), The structure of the polar vortex, *J. Geophys. Res.*, *97*, 7859–7882.

Schoeberl, M. R., M. Luo, and J. E. Rosenfield (1995), An analysis of the Antarctic halogen occultation experiment trace gas observations, *J. Geophys. Res.*, *100*(D3), 5159–5172.

Schoeberl, M., A. Douglass, Z. Zhu, and S. Pawson (2003), A comparison of the lower stratospheric age spectra derived from a general circulation model and two data assimilation systems, *J. Geophys. Res.*, *108*(D3), 4113, doi:10.1029/2002JD002652.

Simmons, A., M. Hortal, G. Kelly, A. McNally, A. Untch, and S. Uppala (2005), ECMWF analyses and forecasts of stratospheric winter polar vortex breakup: September 2002 in the Southern Hemisphere and related events, *J. Atmos. Sci.*, *62*, 668–689.

Tegtmeier, S. (2007), Variationen der stratosphärischen Residualzirkulation und ihr Einfluss auf die Ozonverteilung, Ph.D. thesis, Mathematisch-Naturwissenschaftliche Fakultät der Universität Potsdam, Germany. (Available at http://nbn-resolving.de/urn:nbn:de:kobv:517-opus-12118)

Tegtmeier, S., M. Rex, I. Wohltmann, and K. Krüger (2008), Relative importance of dynamical and chemical contributions to Arctic wintertime ozone, *Geophys. Res. Lett.*, doi:10.1029/2008GL034250, in press.

Uppala, S. M., et al. (2005), The ERA-40 re-analysis, *Q. J. R. Meteorol. Soc.*, *131*, 2961–3012.

van Noije, T., H. Eskes, M. van Weele, and P. van Velthoven (2004), Implications of the enhanced Brewer-Dobson circulation in European Centre for Medium-Range Weather Forecasts reanalysis ERA-40 for the stratosphere-troposphere exchange of ozone in global chemistry transport models, *J. Geophys. Res.*, *109*, D19308, doi:10.1029/2004JD004586.

Weaver, C., A. Douglass, and R. Rood (1993), Thermodynamic balance of three-dimensional stratospheric winds derived from a data assimilation procedure, *J. Atmos. Sci.*, *50*, 2987–2993.

Weber, M., S. Dhomse, F. Wittrock, A. Richter, B. M. Sinnhuber, and J. P. Burrows (2003), Dynamical control of NH and SH winter/spring total ozone from GOME observations in 1995–2002, *Geophys. Res. Lett.*, *30*(11), 1583, doi:10.1029/2002GL016799.

Wohltmann, I., and M. Rex (2008), Improvement of vertical and residual velocities in pressure or hybrid sigma-pressure coordinates in analysis data in the stratosphere, *Atmos. Chem. Phys.*, *8*, 265–272.

————————————

K. Krüger, IFM-GEOMAR, Düsternbrooker Weg 20, 24105 Kiel, Germany.

M. Rex, K. Schoellhammer, and I. Wohltmann, Alfred Wegener Institute for Polar and Marine Research, Telegrafenberg A43, D-14473 Potsdam, Germany.

S. Tegtmeier, Air Quality Research, Environment Canada, 4905 Dufferin Street, Toronto, ON M3H 5T4, Canada. (susann@atmosp.physics.utoronto.ca)